Visualization of Projectile Flying at High Speed in Dusty Atmosphere

Chihiro MASAKI[1*], Yasumasa WATANABE[2], and Kojiro SUZUKI[1]

[1] Department of Advanced Energy, Graduate School of Frontier Sciences,
  The University of Tokyo, 5-1-5 Kashiwanoha, Kashiwa, Chiba 277-8561, Japan.
[2] Department of Aeronautics and Astronautics, Graduate School of Engineering,
  The University of Tokyo, 7-3-1 Hongo, Bunkyo, Tokyo 113-8656, Japan.

E-mail: masaki@daedalus.k.u-tokyo.ac.jp

Abstract. Considering a spacecraft that encounters particle-laden environment, such as dust particles flying up over the regolith by the jet of the landing thruster, high-speed flight of a projectile in such environment was experimentally simulated by using the ballistic range. At high-speed collision of particles on the projectile surface, they may be reflected with cracking into smaller pieces. On the other hand, the projectile surface will be damaged by the collision. To obtain the fundamental characteristics of such complicated phenomena, a projectile was launched at the velocity up to 400 m/s and the collective behaviour of particles around projectile was observed by the high-speed camera. To eliminate the effect of the gas-particle interaction and to focus on only the effect of the interaction between the particles and the projectile's surface, the test chamber pressure was evacuated down to 30 Pa. The particles about 400μm diameter were scattered and formed a sheet of particles in the test chamber by using two-dimensional funnel with a narrow slit. The projectile was launched into the particle sheet in the tangential direction, and the high-speed camera captured both projectile and particle motions. From the movie, the interaction between the projectile and particle sheet was clarified.

1. Introduction

Particle-laden environment is not unusual in space. In deep space missions, a spacecraft may encounter a particle-laden environment during an interplanetary flight, atmospheric flight or travel on the ground. Such encounter may cause serious damage on the spacecraft surface. Generally speaking, the particle-laden environment can be categorized into three situations: the dusty atmosphere, the regolith as packed particles, and the cloud of sparsely scattered particles in the vacuum.

A typical example of the dusty atmosphere will be found on Mars. When an atmospheric probe enters the Martian dusty atmosphere, the flow around the body is significantly influenced by the gas-particle two-phase flow effect [1]. In such case, the aerodynamic heating may be augmented and the damage on the surface may become more severe due to the augmented aerodynamic heating as well as the collision of the dust particles. On those problems, the experimental studies and the numerical studies have been conducted [1]-[3]. The regolith on planets, satellites and asteroids is typical example of the packed particles. For investigation on the interior structure under the ground, impact probe missions have been considered in the past [4]. The behavior of the regolith at the impact will be well described by the soil dynamics and some numerical analysis methods have been developed [5].

The most well-known example of a cloud of sparsely scattered natural particles will be the Saturn's ring. However, such environment appears by an artificial effect. When a spacecraft is approaching to the ground of an asteroid, lots of dust particles must fly upward at high speed, receiving the jet of the landing thruster of the spacecraft [6],[7]. If the same or another spacecraft is flying in the dust cloud, it may encounter the particle cloud at high relative speed. The behavior of the particle cloud is expected to be described by the dynamics of the granular flow. The granular flow has been extensively studied so far [8]. However, most of them consider relatively low speed regimes. The phenomena in high-speed regimes, which may be encountered by a spacecraft, have not been clearly understood, because the granular flow dynamics in high-speed regimes must become much complicated. It includes the crash and abrasion of particles due to high-speed impact among the particles and/or between particles and the spacecraft surface.

Therefore, it is necessary to experimentally clarify the fundamental characteristics of the high-speed granular flow. Specifically, the case that a projectile flies at high-speed in the particle-laden environment must be studied for consideration on possible hazardous situation of a spacecraft.

The experimental method of high-speed inrush into the particle-laden environment was established and changes in the flow field due to differences in the material of the projectile and particles have been observed [9]. In the present study, the shape of the projectile is changed to sphere and observed flow field. In addition, the image processing method for a gray image obtained by experiment is established. The objectives of the present study are as follows:

1) To establish the experimental technique to simulate the high-speed flight of sphere into particle-laden environment by using the ballistic range,

2) To establish the image processing method, to reveal the influence zone of the destruction of particles due to collisions around the projectile, from snapshots of the high-speed camera,

3) To compare the results of image processing with different projectile shapes.

2. Method of experiment

2.1. Ballistic range and optical system

The schematic view of ballistic range is shown in Fig. 1, and the concept of the present experimental setup is shown in Fig. 2. As shown in Fig. 2(a), a sheet of particles is formed in the test chamber, to capture the high-speed flight of a projectile in particle-laden environment from the glass window (Fig.2 (b)). In the case of thick cloud, a recorded image will become integrated one in the viewing direction and the analysis of the image will become difficult to obtain the cross section of the phenomena. A projectile was launched in the tangential direction to the sheet as shown in Fig. 2 (a). The behavior of particles around a projectile was captured by using a high-speed camera, whose viewing direction was normal to the sheet. Such thin planar particle sheet is convenient for observation of the phenomena.

To launch a projectile at a high speed, the ballistic range facility was used. The facility used in this laboratory can launch a projectile with about 10 g mass up to a speed of about 400 m/s, depending on the charged pressure. This facility was used for observation of the shock wave around a body at a free flight and for high-speed collision experiment of a penetrator on an icy target [10]. As shown in Fig. 1, the facility consists of the high-pressure chamber, the barrel tube, the accelerate tube, the adapter, and the test chamber. A projectile is set from the front of the diaphragm section before the experiment. The injection velocity is controlled by appropriately charging the compressed air in the high-pressure chamber. The maximum available pressure is 1 MPa relative to the atmospheric pressure. To eliminate the aerodynamic effect, the test chamber is evacuated down to about 30 Pa before the experiment by using the mechanical booster pump.

To capture the image in the test chamber through the glass window, a high-speed camera Phantom Miro 310 (Nobby Tech. Ltd.) was used. The specifications and the operation parameters are listed in Table 1. In this research, in order to investigate the high-speed collision phenomena, it is necessary to

increase the frame rate and to decrease the exposure time as much as possible. Then the high-intensity metal halide lamp MID-25FC (Lighterrace Inc.) with the maximum power 250 W was used.

As shown in Fig. 2(b), the light enters the test section through the window on the opposite side of the camera. The particles and projectile were illuminated with the backlight configuration. The oil clay in the box of the size $15 \times 20 \times 20$ cm was set ahead of particle sheet. The launched projectile passes through the particle sheet and is finally stopped by the cray.

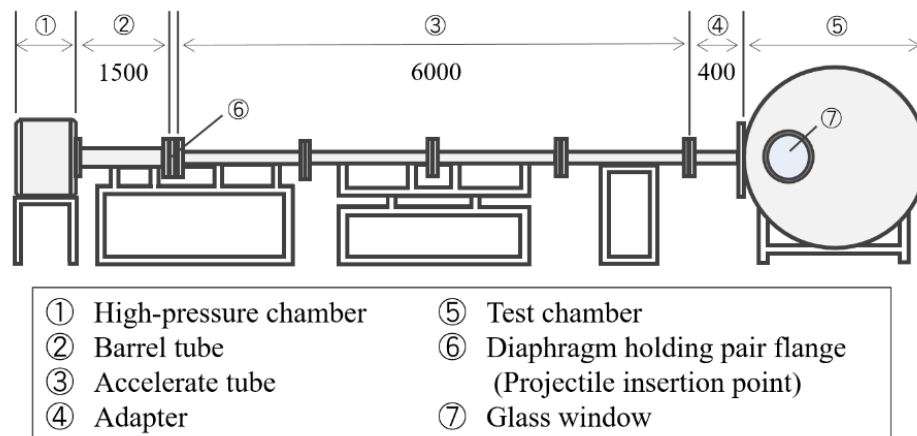| ① | High-pressure chamber | ⑤ | Test chamber |
②	Barrel tube	⑥	Diaphragm holding pair flange
③	Accelerate tube		(Projectile insertion point)
④	Adapter	⑦	Glass window

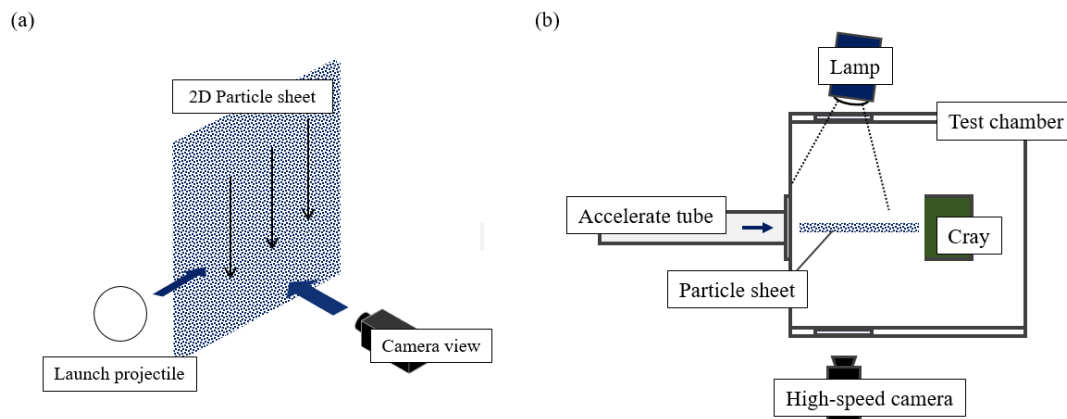Fig. 1. Photograph and conceptual diagram of ballistic range facility.

Fig. 2. Experimental concept and arrangement from the top of test chamber.

Table 1. Specifications and filming parameters of high speed camera.

Specifications	
Brightness resolution	Monochrome (12bit)
Sensitivity (ISO / ASA)	16,000
Minimum exposure time	1.0 μs
Filming parameters	
Image acquisition rate	20,000 pps
Exposure time	1.0 μs
Image resolution	512 x 256 pixels

2.2. Projectiles

The requirements of projectile used in the present experiment were the visibility of the projectile shape, the appropriate size for observation, and the strength to withstand the strong acceleration in the tube. In the present study, spherical shape was selected for a projectile. In our previous study [9], a hemisphere-cylinder was used. The hollow opened to the base of the projectile made the observation of the wake difficult. The outer diameter was the same as the inner diameter of the accelerate tube. Such configuration enables us to launch the projectile without the sabot. The launch without the sabot enhances the stability and repeatability of the experiment, because the sabot often causes a significant disturbance in the attitude and motion of the projectile when it is separated from the projectile. Polycarbonate was selected as a material, because it is strong and has good visibility in the present optical system. To reduce the projectile mass and to obtain high launch velocity, the inside was hollowed out so that the thickness of the body was reduced to about 2 mm. The spherical body was composed of two hemispherical shells, which were tightly glued at their spigot joints. Thanks to the thin shell structure, the mass of the spherical projectile was only about 4.3 g, which was sufficiently light to be launched in the present ballistic range. A photograph of projectile is shown in Fig. 3.

Fig. 3. Photograph of projectile, which diameter is 25.75 mm, mass is 4.3 g, respectively.

2.3. Particle sheet

2.3.1. Particles Considering that the objective of this study is to clarify the fundamental properties of the particle behavior around the projectile, the material and the particle size were selected from a viewpoint of the visibility for the present camera system. Glass beads with about 400 μm diameter was used as brittle particles, and is compatible with the optical system of this work. The appearance and 180 times enlarged images is shown in Fig. 4.
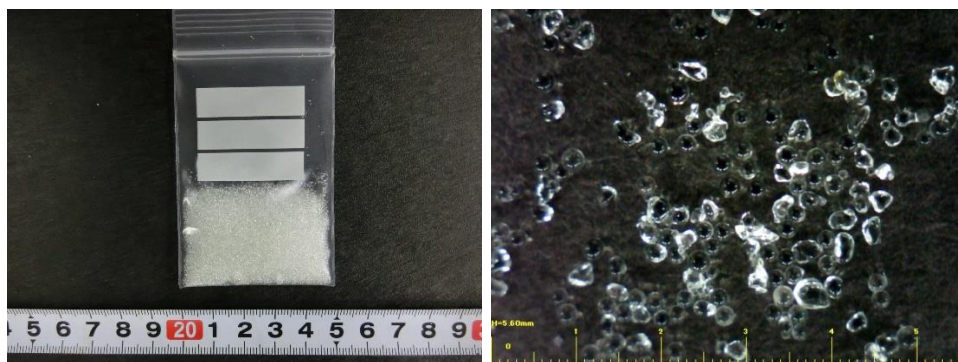

Fig. 4. Photographs of particles (left: appearance, right: 180 times enlarged).

2.3.2. Particle sheet generating device In order to create the particle-laden environment in the test chamber, a device to generate a particle sheet was developed. The uniformity of the particle number density on the sheet is important. Therefore, a mechanism for dropping particle from a slit by the gravitational force was selected. As shown in the Fig. 5 (b), the length of the slit is 100 mm and the gap is 2 mm. Due to the volume of the dust reservoir above the slit, the duration of the particle sheet is about 10 seconds. As shown at the left side of Fig. 5 (a), a shutter at the slit is closed before the experiment, and it is removed by the motor at an arbitrary trigger timing. The terminal speed of the free dropping particles is about 3.0 m/s, which is much smaller than the projectile speed. Consequently, the particles are considered to be floating still in the test chamber in the time scale of the projectile's passage. Using the above device, almost the uniform two-dimensional planar particle sheet was successfully generated. The particle-supply rate and the number density can be calculated. The supply rate is 12.4 g/s. This is calculated from the amount of particles in the funnel and the discharge time. The number density in the particle sheet is estimated about 5×10^8 particles/m^3 from the supply rate and the volume swept by falling particles. These parameters can be changed by particle diameter and material or adjusting slit width.

Photograph of test chamber interior is shown in Fig. 6. Projectile is launched from the right injection port to left. The particle sheet generating system is installed at the top of test chamber. After passing through particle sheet, projectile is stopped by cray.
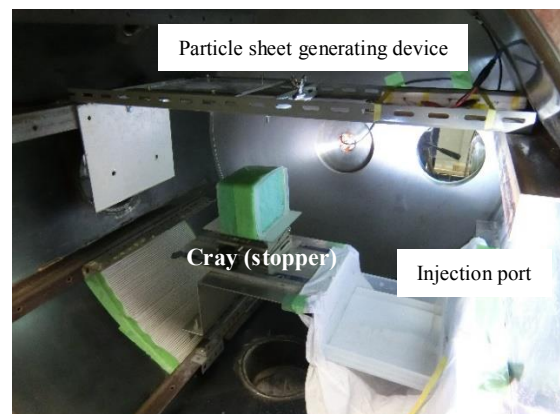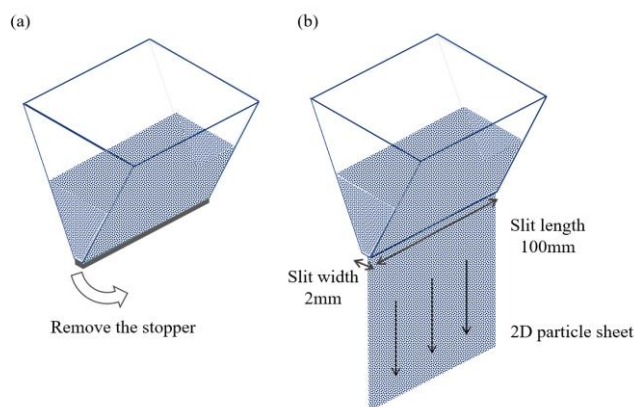

Fig. 5. Illustration of particle sheet generating devise.   Fig. 6. Photograph of test chamber interior.

2.4. Operations and experimental conditions
The experiment was carried out in the following procedure. The test conditions of the present experiments are summarized in Table 2.

  a) Set the projectile from diaphragm holding pair flange (shown Fig. 1),
  b) Evacuate the test chamber down to 30 Pa,
  c) Fill the air into the high-pressure chamber (nominally 0.5 MPa, 1 MPa at the maximum),
  d) Remove the stopper of two-dimensional funnel by the remote control switch, and then start particle sheet generating device,
  e) Launch the projectile and capture the movie by the high-speed camera.

Table 2. Test conditions.

Parameters	Selected condition
High pressure chamber pressure	0.5Mpa
Test chamber pressure	30Pa
Projectile	Polycarbonate sphere
Particle	Glass beads (diameter = 400 μm)

2.5. Image processing

Due to camera specs, the result obtained is grayscale. For consideration, a method for extracting only the region of interest by colorizing the image will be described below.

At first, the brightness of each pixel with 256 levels from black (= 0) to white (= 255) was extracted. Then, the brightness matrix of 512×256 size was obtained from one frame. Next, contour lines with respect to the brightness were drawn. The region with brightness lower than 65 was painted in white to remove the image of the background. Processes and benefits of this image processing are discussed in the next section.

3. Results and discussions

The snapshots of high-speed movie of a projectile flying in a particle sheet are shown in Fig. 7. About 5 frames were extracted from the movie during the period for the projectile to pass through the particle sheet. From these snapshots, the influence of the gas in front of a projectile and that used for acceleration of the projectile in the accelerate tube is thought to be negligible, because the particle sheet does not seem to be disturbed by the air flow. From the angle of the adhesive part of the sphere, the projectile is not rotating. A spherical projectile can ignore posture misalignment more than a hemisphere-cylinder projectile, used in our previous study [9].

In Fig. 7(d)-(f), the particle collision occurs on the projectile surface, and the zone of light emission expands gradually. The emission occurs only in the region where the particles exist and the light is scattered by the presence of particles. If the intensity of the light emission increases with the increase in the local number density of particles, a larger number of particles, some of which may be fine crushed particles, exist in the zone of brighter emission. A black area on the projectile surface is expected to be a shadow of a particle floating between the projectile and the light source.

To estimate the extent of the presence of particles scattered by the projectile, the image processing was made to the original gray scale picture. The process of image processing is shown in Fig. 8. Left picture of Fig. 8 is before subtracting background, right is after subtracted. As seen from these figures, only the particularly bright parts in front of the projectile are extracted.

The snapshots after processing are shown in Fig. 9. From these figures, the influence range is gradually spreading and separated by contour lines. By comparing Fig. 7-(f) and Fig. 9-(f), particles are coming around in the rear part of the projectile. Unlike hemisphere-cylinder projectile, particles are gradually propagated to the back of the projectile. A comparison of images after processing of different projectiles is shown in Fig. 10. In the case of hemisphere-cylinder projectile, the propagation of particles to the wake is stopped at the corner of the cylinder. Also, disorder of posture influences the surrounding propagation. In the case of a sphere, the propagation continues to the rear. As the number of particles going backward increased, the particle density in the front is smaller than that in the case of hemisphere-cylinder projectile.
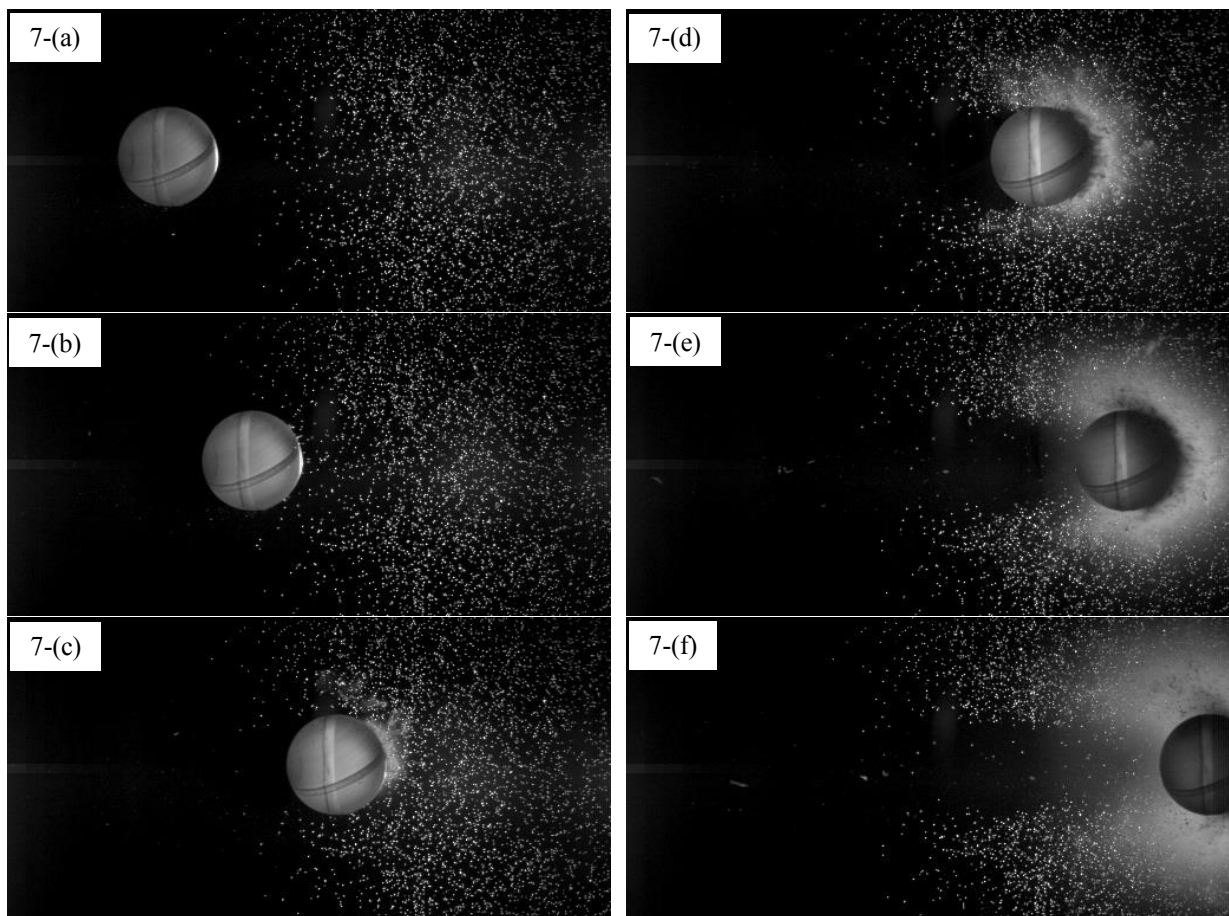
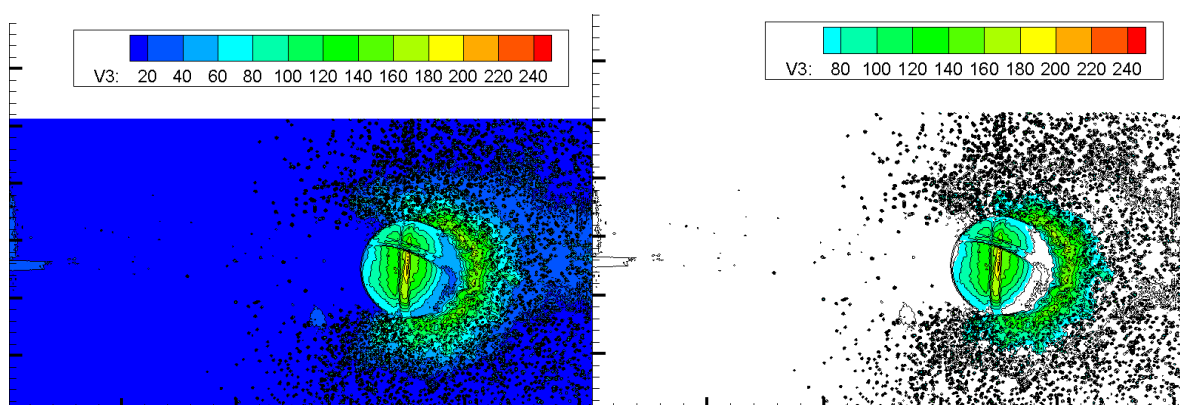Fig. 7. Snapshots of high-speed movie of a sphere flying in particle sheet.

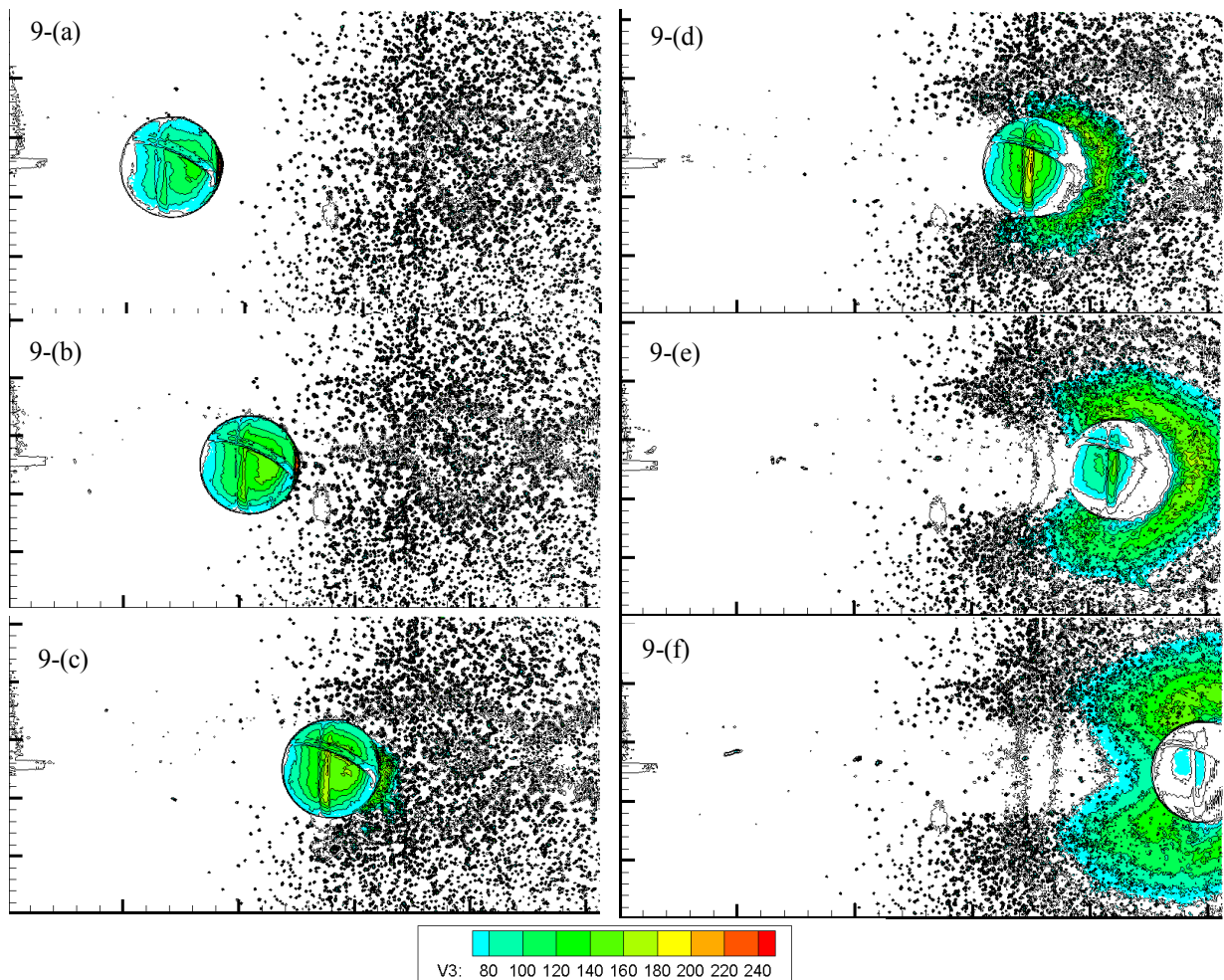Fig. 8. Process of image processing (left: with background, right: background painted in white).

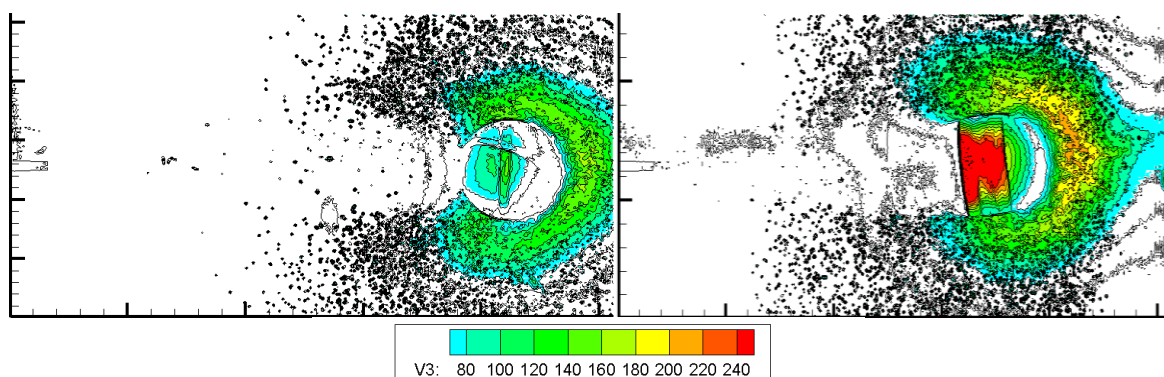Fig. 9. Snapshots of high-speed movie after processing.

Fig. 10. Comparison of different projectile (left: sphere, right: hemisphere-cylinder[11])

4. Conclusions

Considering the hazardous situation of the spacecraft, high-speed collision experiment with spherical projectile and particles was conducted by using ballistic range. The major conclusions are as follows:

1) The experiment of a high-speed flight of a spherical projectile in particle sheet was successfully performed using a ballistic range facility. In order to enable a spherical and lightweight projectile, the

spherical body was composed of two hemispherical shells, which were tightly glued at their spigot joints.

2) To clarify the influence range of particles, image which captured the pattern of the particle behavior around the projectile was processed. By changing grayscale to color and painting white the background, it was possible to extract only the moving range of particles.

3) The image processing results of different projectile shapes were compared and the state of propagation was discussed. In the case of spherical projectile, as the number of particles going backward increased, the particle density in the front is smaller than that in the case of hemisphere-cylinder projectile.

Acknowledgements

References
[1]   Papadopoulos, P., Tauber, M. E. and Chang, I. D.: Heatshield Erosion in a Dusty Martian Atmosphere, J. Spacecraft Rockets, 30(1993), pp. 140-151.
[2]   Vasilevskii, E. B., Chirikhin, A. V., and Osiotsov, A. N.: Heat Transfer to a Stagnation Region of a Blunt Body in a Hypersonic Gas Flow with and Admixture of Solid Particles, Aerothermodynamics for space vehicles, ESA SP, 426(1998), pp.301-307.
[3]   Migita, S. and Suzuki, K.: Numerical Analysis on Dusty Supersonic Shock Layer Flow over a Blunt Body, Transactions of the Japan Society for Aeronautical and Space Sciences, 49(2001), No.566, pp.63-69 (in Japanese).
[4]   Mizutani, H.: Lunar Interior Exploration by Japanese Lunar Penetrator Mission, LUNAR-A, Journal of Physics of the Earth, 43 (1995), No. 5, pp. 657-670.
[5]   Suzuki, K., Abe, T., Higuchi, K., Fujimura, A. and Mizutani, H.: Development of Analysis Model of Penetration Dynamics for Lunar-A Mission, 20th International Symposium on Space Technology and Science(1996), Gifu, 96-i-02V.
[6]   Hirotani. T, et.al.: Spacecraft Contamination by Propulsion Jet Impinging on Dusty Planetary Surface, 32nd Fluid dynamics conference (2000), pp.363-366 (in Japanese).
[7]   Hirotani. T, et.al.: Contamination spacecraft hovering on dusty planet, Symposium on shock wave (2000), pp.589-592 (in Japanese).
[8]   Tomas Schwager, Computational Granular Dynamics: Models and Algorithms, Germany, 2014.
[9]   Masaki. C, Watanabe. Y, and Kojiro. S: Ballistic Range Experiment of Sphere in Dusty Atmosphere, 31st International Symposium on Space Technology and Science(2017), Ehime, 2017-s-10-e.
[10] Namba. K, and Suzuki. K.: Fundamental Study on Penetration Dynamics and Projectile Shape Effect of the Cryo-Penetrator into Icy Object, master's thesis, Department of Aeronautics and Astronautics, The University of Tokyo, 2014 (in Japanese).
[11] Masaki. C, Watanabe. Y, and Kojiro. S: Experimental Study on Granular Flow around a Body Flying in Dens Dust Cloud at Low Atmospheric Pressure, 49th Fluid dynamics conference (2017), 2D06 (in Japanese).